Transverse mass spectra and scaling of hadrons at RHIC and LHC energies

P. K. Khandai[1], P. Sett[2,3], P. Shukla[2,3],[*] and V. Singh[1]

[1]*Department of Physics, Banaras Hindu University, Varanasi 221005, India*

[2]*Nuclear Physics Division, Bhabha Atomic Research Center, Mumbai 400085, India and*

[3]*Homi Bhabha National Institute, Anushaktinagar, Mumbai 400094, India*

arXiv:1205.0648v2 [hep-ph] 29 Jun 2012

Abstract

We present a systematic study of transverse mass (m_T) spectra of mesons and baryons at RHIC and LHC energies. In an earlier study, it was shown that all the mesons produced in p+p and d+Au collisions at $\sqrt{s_{NN}} = 200$ GeV follow m_T scaling while in Au+Au collisions at same energy the mesons with strange and charm quark contents do not follow m_T scaling which can be attributed to medium modifications. We extend this study for baryons produced in all above colliding systems at $\sqrt{s_{NN}} = 200$ GeV. Although all available baryon spectra behave differently from mesons but are found to scale with protons for both p+p and d+Au collisions. In case of Au+Au collisions, the strange baryons behave differently from protons. This study has also been performed on the meson spectra in p+p collisions at 62.4 GeV which lies in between the highest RHIC energy and SPS energy where the m_T scaling was first observed and we arrive at same conclusions as those at 200 GeV. We test the m_T scaling at LHC with the first meson and baryon spectra measured in p+p collisions at 900 GeV and find that the m_T spectra of kaons and ϕ do not scale with pions that well. Here we use all data measured in the mid rapidity region. Proton to pion ratio is studied as a function of m_T, at different energies and for different systems and is found that this ratio for p+p at 900 GeV is quite low from that in p+p collisions at RHIC energies.

Submitted to Physical Review C

---

[*] pshukla@barc.gov.in

I. INTRODUCTION

Heavy ion collisions at relativistic energies are performed to study the properties of matter at high temperature where a phase transition to Quark Gluon Plasma (QGP) is expected. In Au+Au collisions at $\sqrt{s_{NN}} = 200$ GeV at Relativistic Heavy Ion Collider (RHIC), many signals point to the formation of Quark Gluon Plasma (QGP) [1–4]. RHIC continues to study the detailed properties of the strongly interacting matter using p+p, d+Au and Au+Au systems at various colliding energies from 200 GeV down up to 7.7 GeV. First results from Pb+Pb collisions at LHC already giving possible glimpses of QGP from precise measurements of observables such as jets [5] and quarkonia [6, 7]. First measured charged particle spectra from LHC [8] are also available which give the global features of the collisions.

Measurements of transverse momentum spectra for particles emerging from p+p collisions are used as a baseline to which similar measurements from heavy ion collisions are compared to study collective effects. Long ago WA80 collaboration found that the spectral shapes of π and η mesons measured in S + S (200 AGeV) collisions are identical when plotted as a function of m_T [9]. This property is known as m_T scaling and has been extremely useful to extrapolate the meson spectra to unkown regions and to obtain the mesons spectra which are not measured. One application of such analysis is to obtain cocktail of decay products from produced hadrons [4, 10]. Obtaining the integrated yields of hadrons is another important application where m_T scaling can be used.

In an earlier study [11], we found that all mesons follow m_T scaling in p+p and d+Au collision at $\sqrt{s_{NN}} = 200$ GeV, while the mesons with strange and charm quark contents do not follow it in Au+Au collisions at the same energy which can be associated to medium modifications. The more detailed centrality analysis of Au+Au collision reveal that in case of η, the data of all centralities are very well reproduced by m_T scaled pion data. The ratios obtained also remain approximately same for all centralities. For particles, kaon and ϕ, peripheral collision data is better reproduced as compared to central collision data and the ratios also increase as the collision becomes more central. We extend this study for baryons produced in all above colliding systems at $\sqrt{s_{NN}} = 200$ GeV. We study proton and strange baryons such as Λ, Ξ, Ω and their anti-particles. Although all available baryon spectra behave differently from mesons but are found to scale with protons for both p+p and d+Au collisions. In case of Au+Au collisions, the strange baryons behave differently from protons.

This study has also been performed on the meson spectra in p+p collisions at 62.4 GeV. This lies in between the SPS energy and highest RHIC energy. The conclusions at 200 GeV hold at 62.4 GeV. Finally and most importantly we test the m_T scaling at LHC with the first meson and baryon spectra measured in p+p collisions at 900 GeV. It is found that the kaons and the ϕ do not scale that well with pions; but in case of baryon, the m_T scaled curve is in good agreement with the Λ and with the small data set of Ξ. We also study the proton to pion ratio in different systems as a function of energy. It is found that this ratio for p+p at 900 GeV is quite low from that in p+p collisions at RHIC energies.

II. FIT PROCEDURE USING m_T SCALING

In this section, we describe the procedure of fitting of hadron spectra using m_T scaling. To give a good descritption of pion spectra in wide p_T range, the PHENIX collaboration [4, 12–14] used a simple form referred as the modified Hagedorn formula. This formula has been extensively used for p+p, d+Au and Au+Au collisions [11] which in terms of m_T is given by:

$$\begin{aligned} E\frac{d^3N}{dp^3} &= \frac{A}{\left[\exp(-am_T - bm_T^2) + \frac{m_T}{p_0}\right]^n}, \\ &= f_{\pi/p}\left(\sqrt{p_T^2 + m_{\pi/p}^2}\right), \end{aligned} \tag{1}$$

which is close to an exponential form at low p_T and a pure power law form at high p_T. Here $f_{\pi/p}$ is the pion or proton fit function, $m_{\pi/p}$ is the rest mass of pion or proton and A, a, b, p_0 and n are the fit parameters. Then we obtain the spectra of mesons (or baryons) using pion (or proton) fit function as:

$$E\frac{d^3N}{dp^3} = S\ f_{\pi/p}\left(\sqrt{p_T^2 + m_h^2}\right), \tag{2}$$

where m_h is the rest mass of the corresponding meson (or baryon). The factor S is the relative normalization of the meson (or baryon) m_T spectrum to the pion (or proton) m_T spectrum which we obtain by fitting the experimentally measured meson (or baryon) spectrum. We use pion fit function to obtain the m_T spectra of mesons such as ϕ, $K^{\pm}$ and K_s^0 and proton fit function to obtain the m_T spectra of baryons such as Λ, Δ, Ξ and Ω etc.

All the mesons and baryons used in this analysis along with mode of measurement, rapidity and p_T ranges with their references are listed in Table I for p+p and in Table II for

TABLE I. Particles with their mode of measurement, rapidity and p_T ranges for p+p collisions at different energies.

Particle	Mode	p_T range (GeV)	Rapidity range	Reference
p+p collision at $\sqrt{s}$= 62.4 GeV				
π^0	$\gamma\gamma$	0.6-6.7	$\|y\| < 0.35$	PHENIX [17]
$\pi^\pm$	dE/dx	0.3-2.85	$\|y\| < 0.35$	PHENIX [16]
$K^\pm$	dE/dx	0.45-1.95	$\|y\| < 0.35$	PHENIX [16]
p +p collision at $\sqrt{s}$= 200 GeV				
π^0	$\gamma\gamma$	0.6-18.9	$\|y\| < 0.35$	PHENIX [26]
$\pi^\pm$	dE/dx	0.3-2.6	$\|y\| < 0.35$	PHENIX [27]
P	dE/dx	0.468-6.5	$\|y\| < 0.55$	STAR [18]
Λ	P π^-	0.35-4.75	$\|y\| < 0.75$	STAR [19]
Ξ^-	$\Lambda\pi^-$ $\Sigma^-\gamma$	0.67-3.37	$\|y\| < 0.75$	STAR [19]
Ω^-	Λ K^- $\Xi^0\pi^-$ $\Xi^-\pi^0$	1.05-2.83	$\|y\| < 0.75$	STAR [19]
p+p collision at $\sqrt{s}$= 900 GeV				
$\pi^\pm$	dE/dx	0.1-2.5	$\|y\| < 0.8$	ALICE [24]
$K^\pm$	dE/dx	0.2-2.3	$\|y\| < 0.8$	ALICE [24]
P	dE/dx	0.3-2.3	$\|y\| < 0.8$	ALICE [24]
K_s^0	$\pi+\pi-$	0.2-2.7	$\|y\| < 0.8$	ALICE [25]
Λ	P π^-	0.7-3.25	$\|y\| < 0.7$	ALICE [25]
Ξ^-	$\Lambda\pi^-$ $\Sigma^-\gamma$	1.0-2.5	$\|y\| < 0.8$	ALICE [25]

d+Au and Au+Au systems at different energies. The errors on the data are quadratic sums of statistical and uncorrelated systematic errors wherever available. Here we use all data from PHENIX ($|y| < 0.35$), STAR ($|y| < 0.5$, $|y| < 0.75$) and ALICE ($|y| < 0.8$) collaborations. The pion and proton spectra measured in p+p collisions for different energies are fitted using Eq. 1 and the parameters are given in Table III and IV respectively. The parameters for

TABLE II. Particles with their measured decay channels, rapidity and p_T range for d+Au, Au+Au systems at $\sqrt{s_{NN}}$ = 200 GeV.

Particle	Mode	p_T range (GeV)	Rapidity range	Reference
d+Au collision				
P	dE/dx	0.468-3.5	$\|y\| < 0.75$	STAR [20]
Δ^{++}	N π	0.3-1.5	$\|y\| < 0.75$	STAR [21]
Au +Au collision				
P	dE/dx	0.5-10.85	$\|y\| < 0.75$	STAR [22]
Λ	P π^-	0.65-4.75	$\|y\| < 0.75$	STAR [23]
Ξ^-	$\Lambda\pi^-$	0.85-4.75	$\|y\| < 0.75$	STAR [23]
	$\Sigma^-\gamma$			
Ω^-	Λ K^-	1.31-4.0	$\|y\| < 0.75$	STAR [23]
	$\Xi^0\pi^-$			
	$\Xi^-\pi^0$			

TABLE III. The parameters of the Hagedorn distribution obtained by fitting pion spectra measured in p+p collisions at different center of mass energies.

Parameters for pion	$\sqrt{s}$ = 62.4 GeV	$\sqrt{s}$ = 200 GeV [11]	$\sqrt{s}$ = 900 GeV
A (GeV/c)$^{-2}$	7.98 ± 0.42	11.11 ± 0.37	16.32 ± 0.81
a (GeV/c)$^{-1}$	0.137 ± 0.014	0.32 ± 0.03	0.82 ± 0.17
b (GeV/c)$^{-1}$	0.0 (fixed)	0.024 ± 0.011	0.0 (fixed)
p_0 (GeV/c)	1.24 ± 0.026	0.72 ± 0.03	0.43 ± 0.036
n	12.07 ± 0.11	8.42 ± 0.12	6.05 ± 0.28

d+Au and Au+Au collisions are given in Table V and VI respectively for pions and protons. For Au+Au system, data corresponding to four centrality classes namely 10-20 %, 20-40 %, 40-60 % and 60-80 % has been analyzed.

TABLE IV. The parameters of the Hagedorn distribution obtained by fitting proton spectra measured in p+p collisions at different center of mass energies.

Parameters for proton	$\sqrt{s}$ = 62.4 GeV	$\sqrt{s}$ = 200 GeV	$\sqrt{s}$ = 900 GeV
A (GeV/c)$^{-2}$	16.34 ± 5.847	168.87 ± 45.77	305.93 ± 38.69
a (GeV/c)$^{-1}$	0.51 ± 0.108	0.15 ± 0.058	0.283 ± 0.067
b (GeV/c)$^{-1}$	0.0 (fixed)	0.0 (fixed)	0.0 (fixed)
p_0 (GeV/c)	0.87 ± 0.104	0.69 ± 0.029	0.36 ± 0.007
n	11.49 ± 0.77	9.86 ± 0.13	7.17 ± 0.005

TABLE V. The parameters of the Hagedorn distribution obtained by fitting pion spectra measured in d+Au and Au+Au (10-20%) collisions at $\sqrt{s_{NN}}$ = 200 GeV.

Parameters for pion	d+Au system [11]	Au+Au system (10-20% cent.)
A (GeV/c)$^{-2}$	52.30 ± 1.63	1564.36 ± 36.68
a (GeV/c)$^{-1}$	0.24 ± 0.01	0.438 ± 0.007
b (GeV/c)$^{-1}$	0.11 ± 0.01	0.213 ± 0.007
p_0 (GeV/c)	0.77 ± 0.02	0.713 ± 0.004
n	8.46 ± 0.07	8.383 ± 0.017

TABLE VI. The parameters of the Hagedorn distribution obtained by fitting proton spectra measured in d+Au (MB) and Au+Au collisions (for different centralities) at $\sqrt{s_{NN}}$ = 200 GeV.

Parameters for proton	d+Au collision	Au+Au collision for different centralities			
		10-20 %	20-40 %	40-60 %	60-80 %
A (GeV/c)$^{-2}$	0.35 ± 0.10	0.3 ± 0.2	0.98 ± 0.13	0.43 ± 0.13	0.90 ± 0.34
a (GeV/c)$^{-1}$	1.63 ± 0.17	1.07 ± 0.08	0.93 ± 0.16	1.12 ± 0.054	1.16 ± 0.09
b (GeV/c)$^{-2}$	0.0(fixed)	0.0(fixed)	0.0(fixed)	0.0(fixed)	0.0(fixed)
p_0 (GeV/c)	1.09 ± 0.045	2.3 ± 0.12	1.95 ± 0.18	1.78 ± 0.051	1.36 ± 0.05
n	7.06 ± 0.24	10.22 ± 0.21	10.34 ± 0.35	9.48 ± 0.16	9.05 ± 0.19

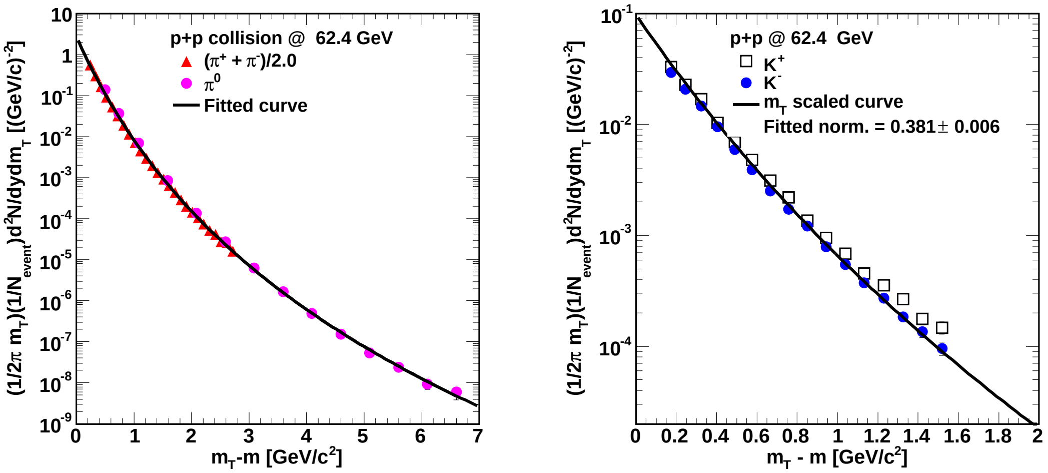

FIG. 1. (Color online) The invariant yield of (a) $\pi^{\pm}$ [16], π^0 [17] and (b) $K^{\pm}$ [16] as a function of m_T for p+p collision at $\sqrt{s}$ = 62.4 GeV.

III. RESULTS AND DISCUSSIONS

Figure (1a) shows the invariant yield of $\pi^{\pm}$ [16], π^0 [17] and (1b) shows the invariant yield of $K^{\pm}$ [16] as a function of m_T measured in p+p collisions at $\sqrt{s} = 62.4$ GeV. Here the data of neutral and charged pion are fitted with modified Hagedorn function shown in solid black curve. The corresponding fit parameters of pion are given in Table III. In case of kaon, the solid line is obtained from pion fit function using m_T scaling; the relative normalization has been used to fit the kaon spectra. There is difference in the measured data for K^+ and K^- and the m_T scaled curve reproduces only K^- well. The relative normalization for kaons are given in Table VII .

Figure 2 shows the invariant yield of different baryons as a function of m_T in p+p collisions at $\sqrt{s} = 200$ GeV. Here the data of proton and anti-proton [18] are fitted with the modified Hagedorn function (shown in solid black curve). The fit parameters are given in Table VI which are used to get the m_T scaled spectra for measured baryons such as Λ, $\bar{\Lambda}$, Ξ^-, $\bar{\Xi}^+$ and Ω^-, $\bar{\Omega}^+$ [19] as shown in figure. The relative normalizations of baryon (given in Table IX) to proton have been obtained by fitting the measured spectra. It is seen that the m_T spectrum of all the baryons are well described by the m_T scaled curve. In case of Λ there are deviations of data from the curve in high p_T region.

The Figure (3a) shows the invariant yield of proton and anti-proton [20] in d+Au system

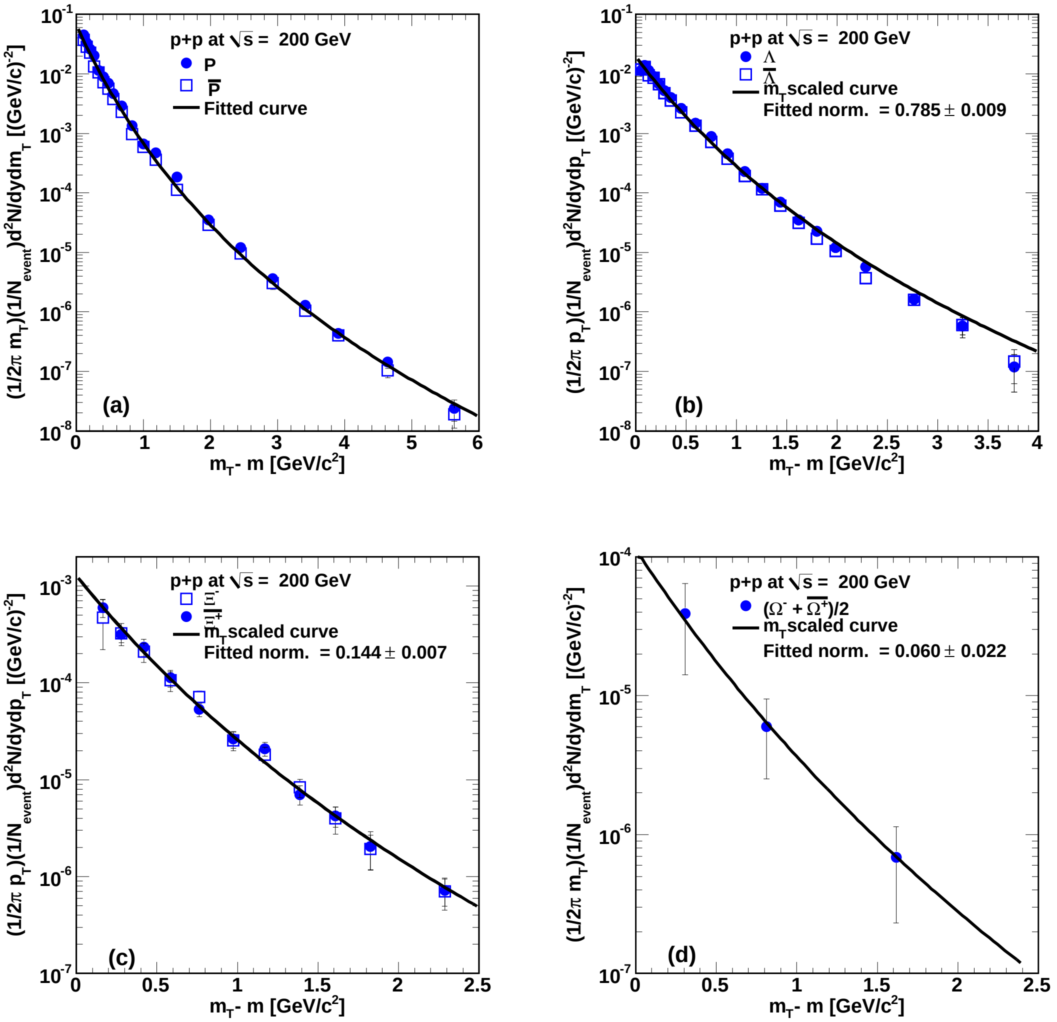

FIG. 2. (Color online) The invariant yield of (a) proton (solid circle), anti-proton (open square) [18], (b) Λ (solid circle), $\bar{\Lambda}$ (open square) [19], (c) Ξ^- (solid circle), $\bar{\Xi}^+$ (open square) [19] and (d) $(\Omega^- + \bar{\Omega}^+)/2$ (solid circle) [19] as a function of m_T for p+p collision at $\sqrt{s} = 200$ GeV.

at $\sqrt{s_{NN}} = 200$ GeV as a function of m_T. The solid black curve is fit function (Eq. 1) the parameters of which are given in the Table VI. The Figure (3b) shows the invariant yield of Δ^{++} [21] as a function of m_T. The solid line is m_T scaled curve; the relative normalisation given in Table IX is obtained by fitting the measured data reproducing the shape of the measured spectrum very well.

Figure 4 shows the invariant yield of proton and anti-proton [20] as a function of m_T for Au+Au collsion at $\sqrt{s_{NN}} = 200$ GeV for different centralities. The solid black curves are

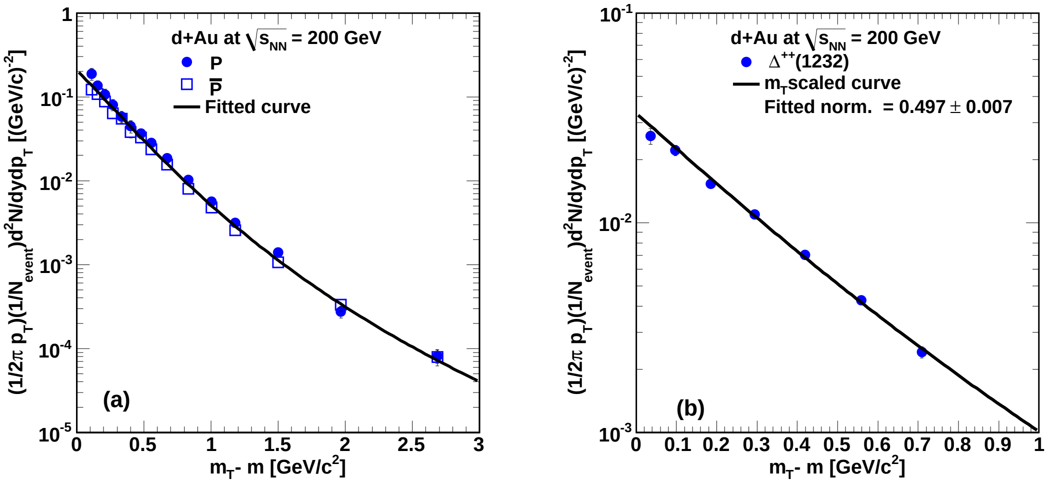

FIG. 3. (Color online) The invariant yield of (a) proton (solid circle), anti-proton (open square) [20] and (b) Δ^{++} baryons [21] as a function of m_T for d+Au collision at $\sqrt{s_{NN}}$ = 200 GeV.

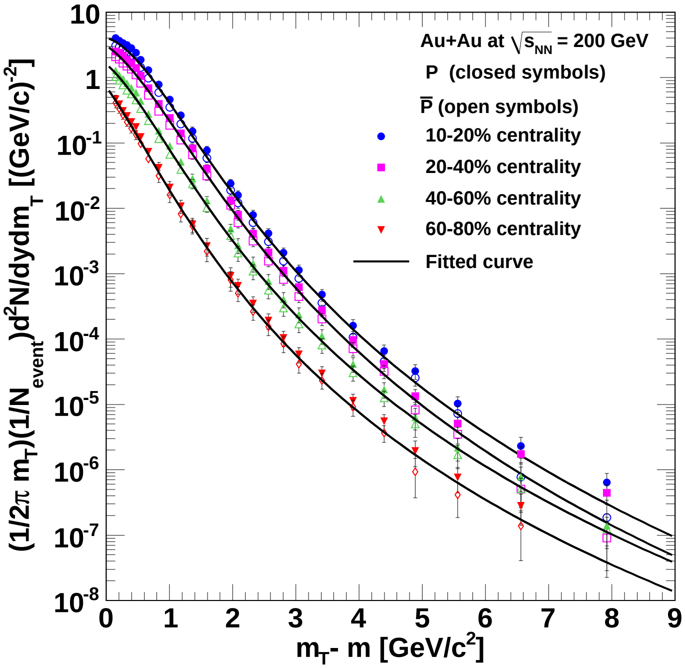

FIG. 4. (Color online) The invariant yield of proton (closed symbols) and anti-proton (open symbols) [22] as a function of m_T in Au+Au collisions at $\sqrt{s_{NN}}$ = 200 GeV for different centralities. The solid lines are Hagedorn fit function.

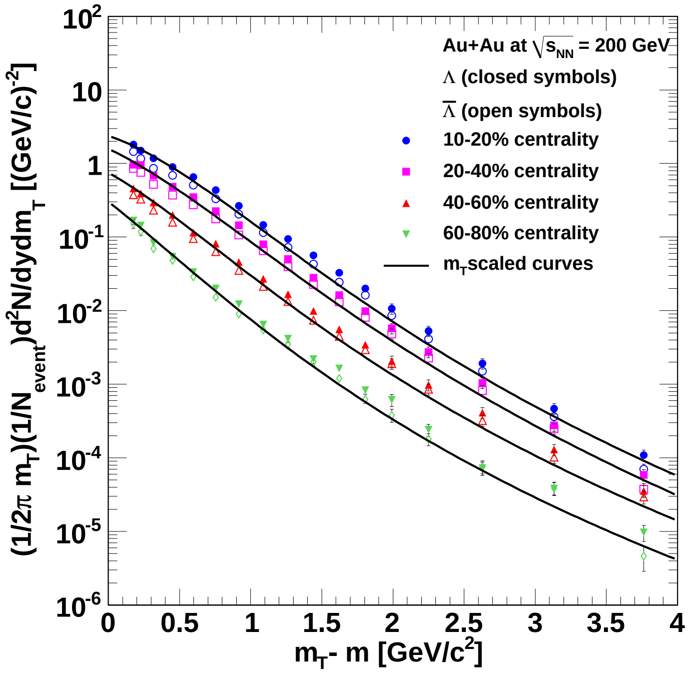

FIG. 5. (Color online) The invariant yield of Λ (closed symbols) and $\bar{\Lambda}$ (open symbols) [23] as a function of m_T in Au+Au collisions at $\sqrt{s_{NN}}$ = 200 GeV for different centralities. The solid lines are obtained using m_T scaling; the relative normalization has been used to fit the measured spectra.

the fitted modified Hagedorn functions with parameters given in Table VI. Figure 5 shows the invariant yield of Λ and $\bar{\Lambda}$ [23] for different centralities as a function of m_T for Au+Au collision at $\sqrt{s_{NN}}$ = 200 GeV. The solid black curves are the m_T scaled curves obtained from the proton spectra of corresponding centralities with a fitted normalization given in Table IX. Figure 6 shows the invariant yield of Ξ and $\bar{\Xi}$ [23] for different centralities as a function of m_T for Au+Au collision at $\sqrt{s_{NN}}$ = 200 GeV. The solid black curves are the m_T scaled curves obtained from the proton spectra of corresponding centralities with a fitted normalization given in Table IX. Here we see that, in both the cases for Λ, $\bar{\Lambda}$ and Ξ^-, $\bar{\Xi}^+$, the experimental data are in good agreement with the m_T scaled curve for the most peripheral centrality bin. But for other centralities, the nature of the m_T scaled curves are different from the shape of data. Same obeservation is made from Figure 7 which shows the invariant yield of Ω [23] as a function of m_T for Au+Au collision at $\sqrt{s_{NN}}$ = 200 GeV.

Figure (8a) shows the invariant yield of $\pi^{\pm}$ [24] as a function of m_T for p+p collision at

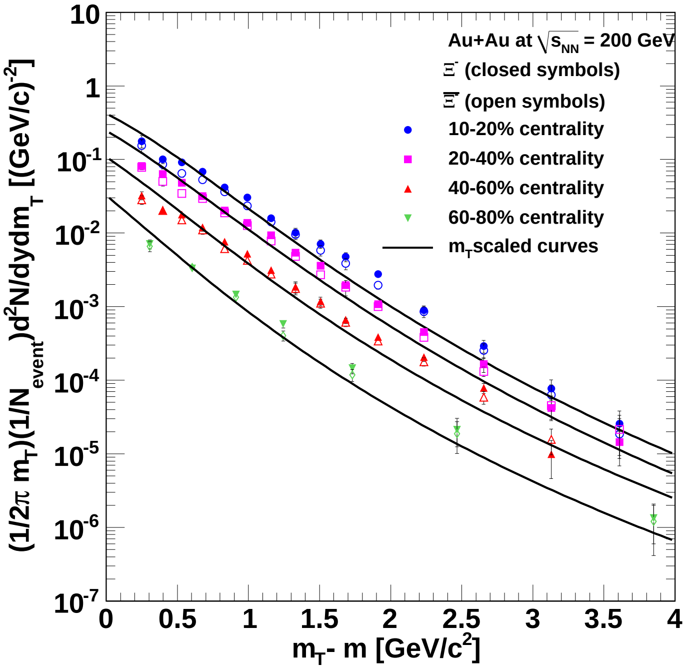

FIG. 6. (Color online) The invariant yield of Ξ^- (closed symbols) and $\bar{\Xi}^+$ (open symbols) [23] as a function of m_T in Au+Au collisions at $\sqrt{s_{NN}}$ = 200 GeV for different centralities. The solid lines are obtained using m_T scaling; the relative normalization has been used to fit the measured spectra.

$\sqrt{s}$ = 900 GeV. The solid black curve is fit function (Eq. 1) whose parameters are given in the Table III. Figures 8 (b), (c) and (d) show the invariant yields of $K^{\pm}$ [24], K^0_S [25], and ϕ [25], respectively as a function of m_T. The solid black curves are the m_T scaled curves obtained from the pion spectrum with a fitted normalization given in Table VII. From this we clearly see that the m_T scaled curves do not reproduce mesons for p+p at 900 GeV that well.

The Figure 9 shows the invariant yields of proton and anti-proton [24] as a function of m_T for p+p collision at $\sqrt{s}$ = 900 GeV. The solid black curve is the fitted modified Hagedorn function with parameters given in Table IV. The Figures 9 (b) and (c) show the invariant yields of Λ [25] and Ξ [25]. The solid black curves are the m_T scaled curves obtained from the proton spectra with fitted normalizations given in the Tabe VIII. Here the m_T scaled curve is in good agreement with Λ and with small data set of Ξ at $\sqrt{s}$ = 900 GeV.

Figure 10 shows the invariant yields of proton (P), anti-proton ($\bar{P}$) and pion (π) as a

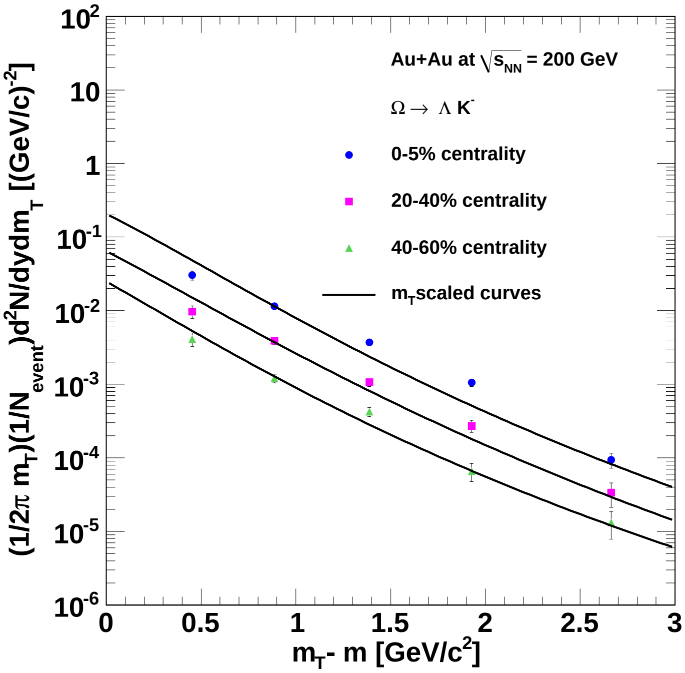

FIG. 7. (Color online) The invariant yield of Ω (closed symbols) [23] as a function of m_T in Au+Au collisions at $\sqrt{s_{NN}} = 200$ GeV for different centralities. The solid lines are obtained using m_T scaling; The Relative normalization has been used to fit the measured spectra.

function of m_T for p+p collisions at $\sqrt{s} = 62.4$, 200 and 900 GeV and for Au+Au collisions (10-20% centrality) at $\sqrt{s_{NN}} = 200$ GeV along with their fit functions obtained from Eq. 1. The shapes of pions and protons m_T spectra are different for all systems at all energies. In comparision to the proton and pion production at low energies (e.g. 62.4 and 200 GeV), the proton production is less as compared to the pion production at 900 GeV.

Figure 11 shows the ratio of proton to pion (p/π) (obtained from the fit functions in Figure 10) vs m_T for p+p collisions at $\sqrt{s} = 62.4$, 200 and 900 GeV and for Au+Au collisions (10-20% centrality) at $\sqrt{s_{NN}} = 200$ GeV. It is seen that for p+p collisions, the shape of p/π curves are same at 62.4, 200 and also at 900 GeV, but the ratio of p/π is very small at $\sqrt{s_{NN}} = 900$ GeV. The enhancement of p/π ratio at intermediate m_T in Au+Au is understood in terms of recombination model [30].

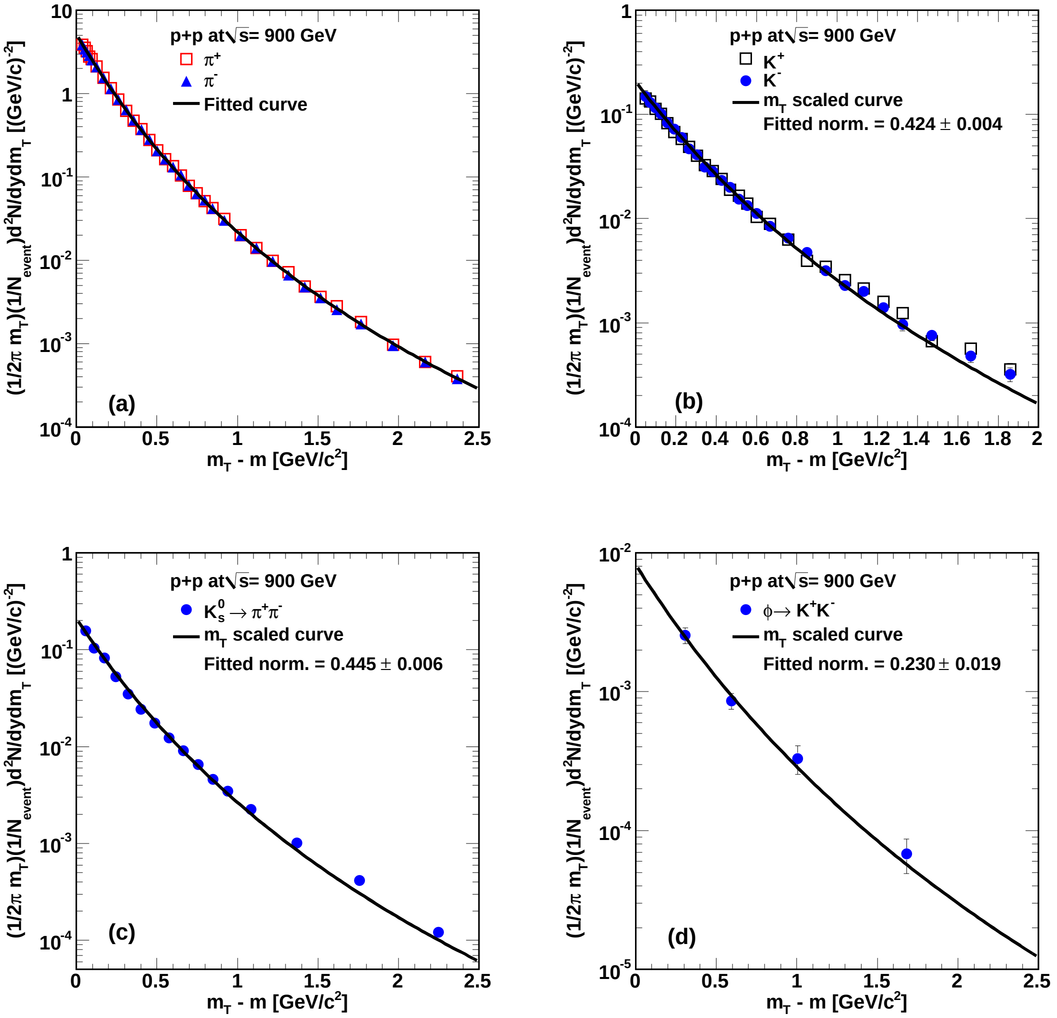

FIG. 8. (Color online) The invariant yield of (a) $\pi^{\pm}$ (closed triangle) [24], (b) K$^{\pm}$ (open square, solid circle) [24], (c) K^0_S (solid circle)[25] and (d) ϕ (solid circle) [25] as a function of m_T for p+p collision at $\sqrt{s}$ = 900 GeV. The solid lines are obtained using m_T scaling.

TABLE VII. The relative normalization (S) of mesons obtained by fitting the m_T scaled spectra with the measured spectra for p+p collisions at $\sqrt{s}$ = 62.4, 200 and 900 GeV.

S	$\sqrt{s}$ = 62.4 GeV	$\sqrt{s}$ = 200 GeV From [11]	$\sqrt{s}$ = 900 GeV
K/π	0.38 ± 0.02	0.422 ± 0.014	0.424 ± 0.02
K^0_S/π			0.44 ± 0.02
ϕ/π		0.233 ± 0.013	0.23 ± 0.02

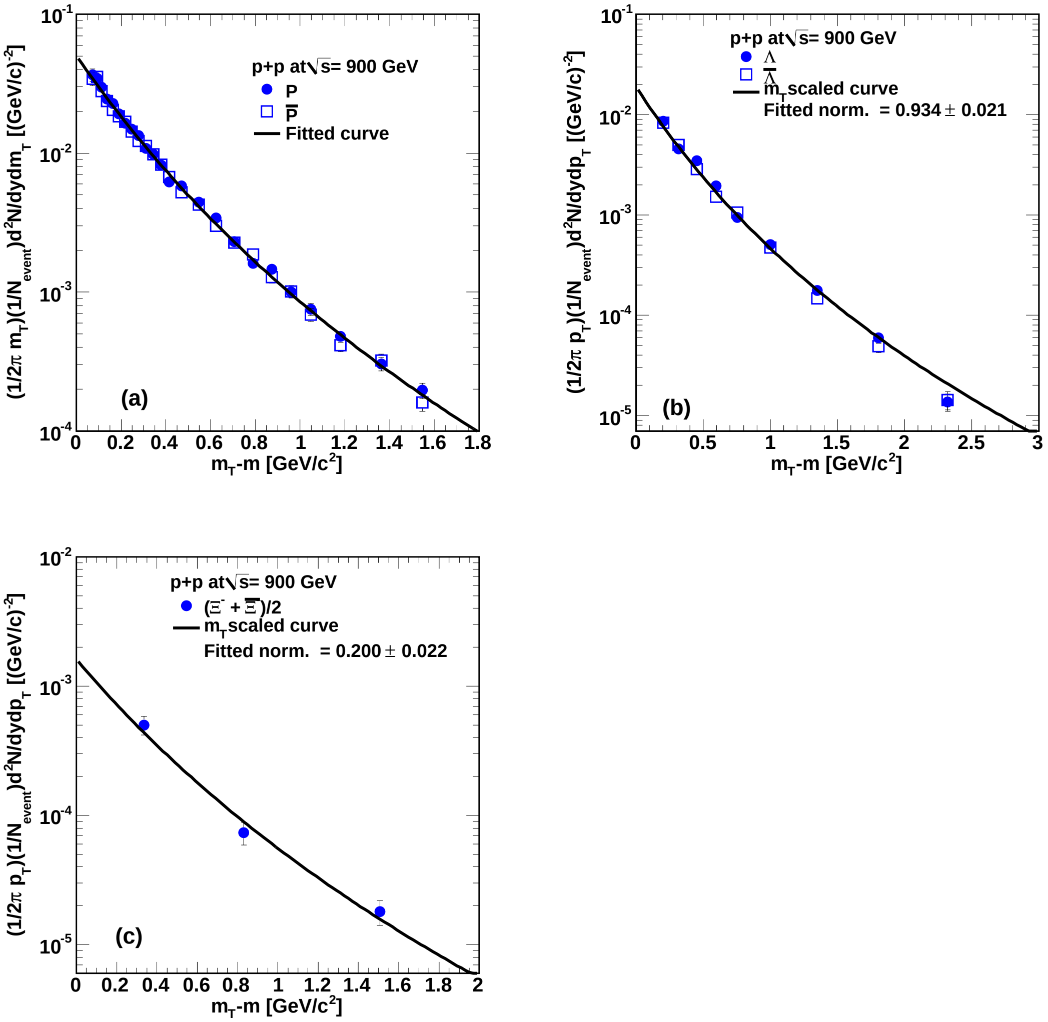

FIG. 9. (Color online) The invariant yield of (a) proton (solid circle), anti-proton (open square) [24], (b) Λ (solid circle), $\bar{\Lambda}$ (open square) [25] and (c) Ξ (solid circle) [25] as a function of m_T for p+p collision at $\sqrt{s}$ = 900 GeV. The solid lines are obtained using m_T scaling.

TABLE VIII. The relative normalization (S) of baryons obtained by fitting the m_T scaled spectra with the measured spectra for p+p collisions at different center of mass energies.

S	$\sqrt{s}$ = 200 GeV	$\sqrt{s}$ = 900 GeV
Λ/p	0.785 ± 0.021	0.93 ± 0.2
Ξ/p	0.14 ± 0.03	0.2 ± 0.02
Ω/p	0.060 ± 0.022	

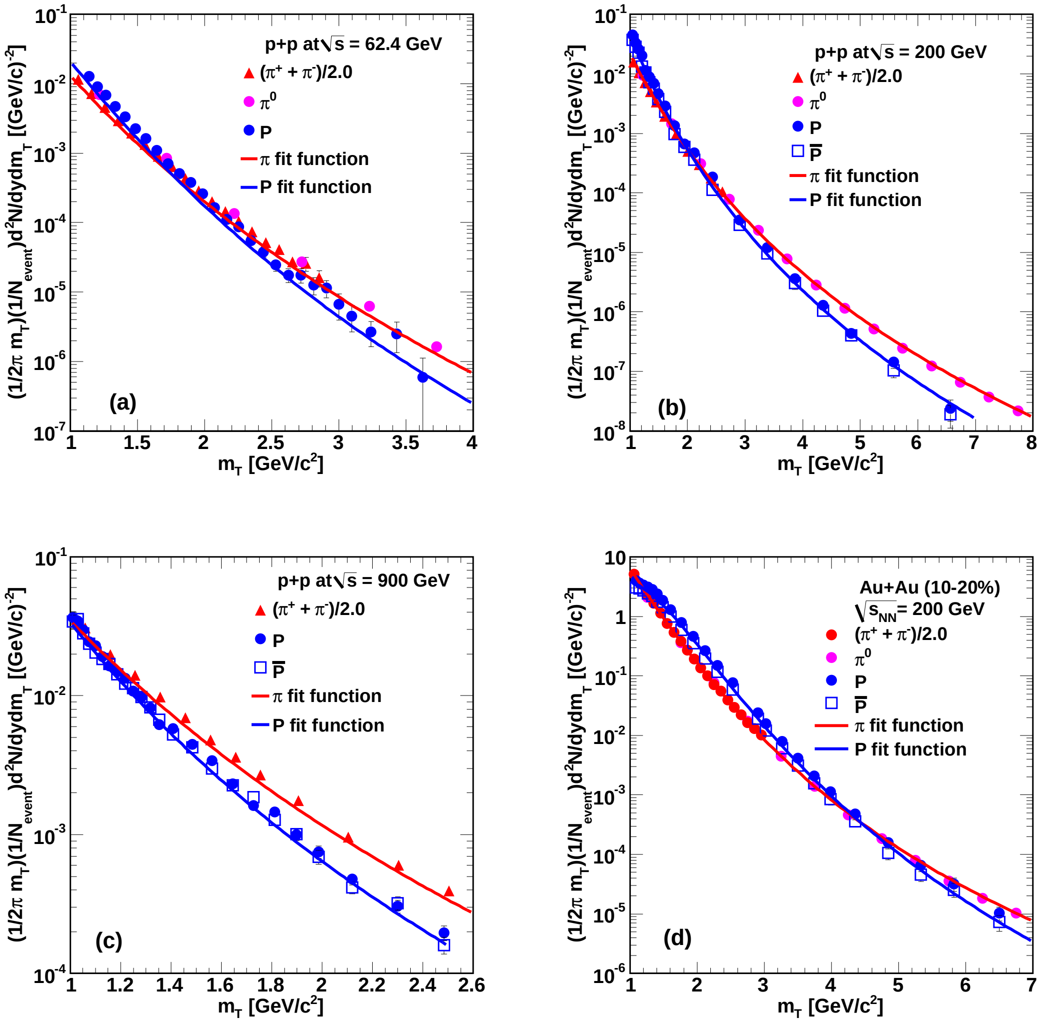

FIG. 10. (Color online) The invariant yields of proton, anti-proton, $\pi^{\pm}$ and π^0 as a function of m_T for (a) p+p at $\sqrt{s}$ = 62.4 GeV [16, 17], (b) p+p at $\sqrt{s}$ = 200 GeV [18, 26, 27], (c) p+p at $\sqrt{s}$ = 900 GeV [24], (d) Au+Au (for 10-20% centrality) at $\sqrt{s_{NN}}$ = 200 GeV [22, 28, 29]. The solid lines show the modified Hagedorn fit function drawn over proton and pion.

IV. CONCLUSION

In summary, we have made a systematic study of transverse mass spectra of mesons and baryons at RHIC and LHC energies. For p+p and d+Au collision at $\sqrt{s_{NN}}$ = 200 GeV the baryon m_T spectra scale with proton m_T spectrum just like all meson spectra scale with pion spectra. In p+p 200 GeV, m_T scaling reproduce data well for all the baryons except Λ as there is a disagreement at high p_T points. In case of Au+Au collisions, the strange

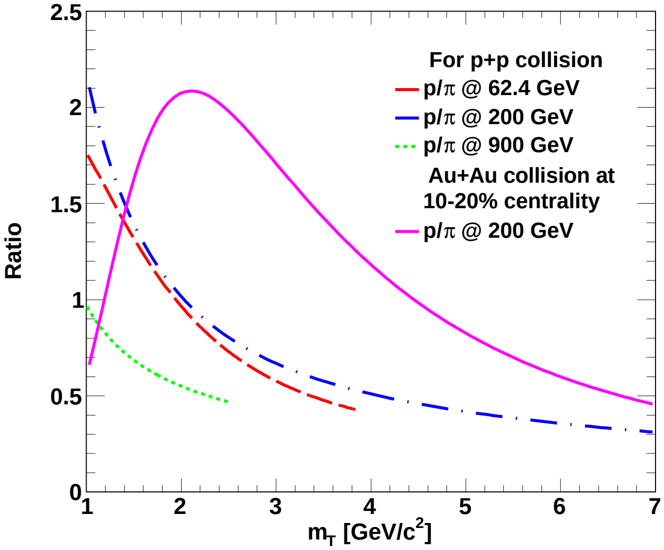

FIG. 11. (Color online) The ratio of proton fit function to the pion fit function (p/π) as a function of m_T for p+p collisions at different energies and Au+Au collisions (10-20% centrality) at 200 GeV.

TABLE IX. The relative normalization (S) of baryons obtained by fitting the m_T scaled spectra with the measured spectra for different collision systems at $\sqrt{s_{NN}} = 200$ GeV.

S	p+p collision	d+Au collision	Au+Au collision for different centralities			
			10-20%	20-40 %	40-60 %	60-80 %
Λ/p	0.785 ± 0.021		0.70 ± 0.09	0.70 ± 0.09	0.7 ± 0.2	0.75 ± 0.28
Ξ/p	0.140 ± 0.030		0.18 ± 0.02	0.18 ± 0.02	0.18 ± 0.05	0.17 ± 0.06
Ω/p	0.060 ± 0.022		0.16 ± 0.008(0-5%)	0.13 ± 0.01	0.12 ± 0.03	
Δ/p		0.497 ± 0.016				

baryons behave differently from protons for all centralities but there is better agreement in the two for peripheral collisions. This study has also been performed on the meson and baryon spectra in p+p collisions at 62.4 GeV which lies in between the highest RHIC energy and SPS energy where the m_T scaling was first observed and we find that the m_T scaling of mesons work at 62.4 GeV (Baryon data at 62.4 GeV is not available). We test the m_T scaling at LHC with the first meson and baryon spectra measured in p+p collisions at 900 GeV and find that the m_T spectra of kaons and ϕ do not scale with pions that well. At

900 GeV, Λ is produced well by m_T scaling where as the Ξ spectrum is reproduced well within the limited availability of data points. The shapes of pions and protons m_T spectra are different at all energies. Proton to pion ratio is studied at different energies (using fit functions) and for different systems and is found that for p+p collisions, the behaviour of p/π curves are similar at 62.4, 200 and also at 900 GeV. It will be interesting to have such study at higher energies such as 2.76 TeV and 7 TeV, once the data tables are available. More comprehensive measurements at lower energies such as 62.4 GeV will benifit to draw a systematic picture of hadron production as a function of energy.

V. ACKNOWLEDGEMENTS

We acknowledge the financial support from Board of Research in Nuclear Sciences (BRNS) for this project. We thank S. Kailas, A. Chatterjee and A. K. Mohanty for fruitful discussions.

---

[1] I. Arsene et. al. (BRAHMS), Nucl. Phys. A**757**, 1 (2005); B. B. Back et. al. (PHOBOS), Nucl. Phys. A**757**, 28 (2005); J. Adams et. al. (STAR), Nucl. Phys. A**757**, 10 (2005); K. Adcox et. al. (PHENIX), Nucl. Phys. A**757**, 184 (2005).
[2] S. S. Adler et al. (PHENIX), Phys. Rev. Lett. **94**, 082302 (2005).
[3] A. Adare et al. (PHENIX), Phys. Rev. Lett. **104**, 132301 (2010).
[4] A. Adare et al. (PHENIX), Phys. Rev. C**81**, 034911 (2010).
[5] Chatrchyan S. et al. (CMS), Phys. Rev. C**84**, 024906 (2011).
[6] Chatrachyan S. et al. (CMS) Phys. Rev. Lett. **107**, 052302 (2011).
[7] Chatrchyan S. et al. (CMS) arXiv:1201.5069 [nucl-ex] (2012).
[8] Chatrchyan S. et al. (CMS) JHEP 1108 086 (2011).
[9] R. Albrecht et. al. (WA80 collaboration), Phys. Lett. B**361**, 14 (1995); arXiv:hep-ex/9507009.
[10] A. Adare et al. (PHENIX), Phys. Lett.B**670**, 313 (2009).
[11] P. K. Khandai, P. Shukla and V. Singh, Phys. Rev. C**84**, 054904 (2011).
[12] A. Adare et al. (PHENIX), arXiv:1005.1627(2010).
[13] A. Adare et al. (PHENIX), Phys.Rev.D**83**, 052004 (2011).

[14] S. Kelly (PHENIX), J. Phys. G**30**, S1189 (2004).

[15] K. Adcox et al. (PHENIX), Phys. Rev. Lett **88**, 192303 (2002).

[16] A. Adare et al. (PHENIX), Phys. Rev. C**83**, 064903 (2011).

[17] A. Adare et al. (PHENIX) Phys. Rev. D**79**, 012003 (2009).

[18] B. I. Abelev et al. (STAR), Phys. Rev. C**75**, 64901 (2007).

[19] J. Adams et al. (STAR), Phys. Lett. B**637**, 161 (2006).

[20] J. Adams et al. (STAR), Phys. Lett. B**616**, 8 (2005).

[21] J. Adams et al. (STAR), Phys. Rev. C**78**, 44906 (2008).

[22] J. Adams et al. (STAR), Phys. Rev. Lett. **97**, 132301 (2006).

[23] J. Adams et al. (STAR), Phys. Rev. Lett. **98**, 62301 (2007).

[24] K. Aamodt et al. (ALICE) Eur. Phys. J. C**71**(6), 1655 (2011).

[25] K. Aamodt et al. (ALICE) Eur. Phys. J. C**71**(3), 1594 (2011).

[26] A. Adare et al. (PHENIX), Phys. Rev. D**76**, 051106(R) (2007).

[27] S. S. Adler et al. (PHENIX), Phys. Rev. C**74**, 024904 (2006).

[28] A. Adare et al. (PHENIX), Phys. Rev. Lett. **101**, 232301 (2008).

[29] S. S. Adler et al. (PHENIX), Phys. Rev. C**69**, 034909 (2004).

[30] R. Fries, V. Greco and P. Sorensen, arXiv:0807.4939v1 [nucl-th] (2008).